Journal of Inorganic and Organometallic Polymers and Materials (2021) 31:4480–4490
https://doi.org/10.1007/s10904-021-02068-0

Developing the NiO/$CuTiO_3$/ZnO Ternary Semiconductor Heterojunction for Harnessing Photocatalytic Activity of Reactive Dye with Enhanced Durability

G. Divya[1] · S. Sivakumar[1] · D. Sakthi[2] · A. Priyadharsan[2] · V. Arun[2] · R. Kavitha[3] · S. Boobas[4]

Received: 29 April 2021 / Accepted: 6 July 2021 / Published online: 21 July 2021

Abstract
Solar active ternary NiO/$CuTiO_3$/ZnO semiconductor heterojunction were developed by alcoholic dispersion technique. As prepared ternary system and parent photocatalysts were analyze crystalline phase, surface morphology, light absorbance property, electron hole accusation parting and significant functional groups by means of specific physicochemical feature measurements. From the results, enhanced visible light photo mineralization, superior efficiency of charge carriers separation and better photocatalytic degradation of reactive orange 30 were confirmed for ternary NiO/$CuTiO_3$/ZnO semiconductor heterojunction. Hydroxyl radical in the radical trapping experiments confirmed the photocatalytic degradation, which plays an important role in removal of hazardous dye from industrial effluents. This work demonstrates that synergetic effect of $CuTiO_3$ and NiO in which it proves to be a good option for recovering the consumption of visible light of ZnO-based materials in the ternary hybrid conduction bands.

Keywords NiO/$CuTiO_3$/ZnO · Ternary composites · Reactive orange 30 · Photocatalytic efficiency and natural sunlight

1 Introduction

As the water was insufficient and effluents from the industries also makes the water resources to pollute which needs treatment to get solutions from pollutants. Aniline has many applications in the manufacture of polymer herbicides, pharmaceuticals, polyurethane, and dyes. This type of compound present in the wastewater from textile industries becomes toxic and cancer-causing material which affects the public health and natural world. There is a need of removal of this pollutants from the surroundings were we can use lot of methods for the waste water treatment including membrane filtration, adsorption, ozonation, biological treatment, and electrolysis [1–6]. In the recent research a photocatalytic method was used for wastewater treatment [7–9].

Photochemical sewerage treatments have been organized using photocatalyst such as metal oxides (TiO_2 [10], ZnO [11, 12]), sulfides [13], and oxynitrides [14] because of its inexpensive, well organized and their stability. ZnO has been used widely in environmental treatments has it can be used in broad temperature range [15–18]. ZnO also has some drawbacks such as un-uniformed dispersal, difficult to fix, and it can be easily recombine the photogenerated electron–hole pairs [19]. From the intensive statement, ZnO might only absorbed by ultra violet irradiation and resist the visible light source.

Moreover, we need to change these difficult behavior, introduced various strategies in the way of surface modification techniques. Among the potential treatments, ternary heterojunctions are formed by coupling of ZnO with one or more narrow band semiconductors. The ternary heterojunctions helps in the formation of charge separation, increasing life of the charge carrier, and the ZnO optical reaction range has been extended [19–21]. [19] Peng et.al., developed A novel Pt/CeO_2/ZnO ternary composite is synthesized via two simple procedures of hydrothermal and

✉ S. Sivakumar
sivabanu8494@gmail.com

[1] Department of Chemistry, E. R. K Arts and Science College, Dharmapuri, Tamil Nadu, India

[2] Department of Physics, E. R. K Arts and Science College, Dharmapuri, Tamil Nadu, India

[3] Department of Chemistry, Shri Sakthikailassh Women's College, Salem, Tamil Nadu, India

[4] Department of Physics, Sri Vasavi College (Govt. Aided), Erode, Tamil Nadu, India

photoreduction. The novel Pt/CeO_2/ZnO ternary composite showed enhanced photocatalytic activity is due to redox cycle of $Ce^{4+} \leftrightarrow Ce^{3+}$, the effective interface between ZnO and CeO_2 as well as the electron transfer action of Pt nanoparticles. Ali İmran Vaizoğullar et. al., [20] fabricated ternary CdS/MoS_2/ZnO composites showed higher photoelectrochemical and photocatalyic activity due to prolonged lifetime of charge it carries, crystalline defect and surface plasmon resonance of CdS. Heterostructured ternary nanocomposites of silver doped magnetites with ZnO (Z) synthesized by Avis Tresa Babu et. al., [21] Hetero structured and Ag doped nano composites exhibited better degradation efficiency of malagite green & methylene blue. This nanocomposites also exhibited strong antibacterial activity with greater inhibition zones due to the synergistic effect of silver and magnetite nanoparticles.

NiO is the inexpensive semiconducting oxides used in photocatalytic applications. The reason is efficiently suppress the electron–hole recombination and enhance the degradation kinetics by composing with ZnO because of the difference in band gap energy [22, 23]. ZnO–NiO composite plays important photocatalytic systems were the researchers indicated the property development and efficiency by compositing of these materials [24–26].

CuO is one of the fabricating p-n heterojunctions with ZnO, because it has stable property, narrow band gap, visible light reaction, and non-toxicity. CuO/ZnO p-n heterojunction has been reported their photocatalytic activity [27, 28]. Though, ZnO binary composite photocatalyst have a few defects. It cannot photo degrade a few hazard pollutants in wastewater, in particular halogenated hydrocarbons. Moreover, the degradation efficiency decreases apparently when there is a multiplicity of pollutants in wastewater. The structure of ternary nanocomposites lead to superior photocatalytic performance by multistep charge transfer and promote the charge separation, by comparing with binary [29–31].

Based on the above background conversation, incorporated using first row transition metal oxide and provoskite type metal tittanate coupled on ZnO semiconductor, NiO/$CuTiO_3$/ZnO ternary composites were fabricated by a simple dispersion method. The NiO/$CuTiO_3$/ZnO ternary composites exhibit much higher photocatalytic activity and excellent cycling performance for removal of Reactive Orange 30 in water under solar light irradiation.

2 Experimental Work

This work deals with the process of preparation of catalyst, characterization techniques and the experimental set-up used for the carrying out the photocatalytic degradation process.

2.1 Chemicals Used

Reactive Orange 30 a widely used in textile dye with dichloroquinoxaline groupand azo group supplied by Vexentdyeaux India Pvt. Ltd, Mumbai (Minimum dye content 70%) were used for photocatalytic degradation studies.

Chemical formula: $C_{29}H_{13}Cl_2N_5O_{13}S_4Na_4$
Molecular weight: 930.56
Water solubility: 70 g/L at 293 k
λ_{max}: 422 nm

Zinc chloride (98%), Sodium bicarbonate (99%) and Copper acetate (GR), Nickel chloride (GR) were supplied by Merck India Pvt. Ltd; dye solutions for photocatalytic studies were prepared in double distilled water. NaOH and HCl were used for modifying the pH of the solutions. $K_2Cr_2O_7$ (AR), Ag_2SO_4 (GR), $HgSO_4$ GR) 99% Ferroin (GR) and HCl were used for Chemical Oxygen Demand analysis. Isopropanol, benzoquinone, ammonium oxalate and terephthalic acid used as scavengers in deduction of active species measurement.

2.2 Preparation of ZnO Photocatalyst

In the preparation of ZnO, 10 g of zinc chloride were dissolved in 100 ml of double distilled water. To that solution 6.2 g of sodium bicarbonate was added and then vigorous stirring until the precipitate was formed well. The NaCl was removed from the precipitate, washed by distilled water more than three times. Then the precipitate was dried at 100 °C to remove the water. The solid obtained after drying was grinded in an agate mortar and transferred into a ceramic crucible. It was calcined at 500 °C for 4 h.

2.3 Preparation of $CuTiO_3$ Microstructure

$CuTiO_3$ microstructure was synthesized by using micelle surfactant method. In typical synthesis 0.005 mol metal salts (Copper source) and 0.005 mol of $TiCl_4$ has been dissolved in 100 ml of distilled water, which reacts with 0.01 molar of Sodium hydroxide to formed nickel hydroxide precipitate. In additional aqueous micelle solution of CetylTrimethylammonium Bromide was added to over the solution, after the material was refluxed for 12 hrs at 75 °C. The filtrate was removed and the precipitate was washed with water 3 to 4 times, further it was dried in air at 100 °C for ten hours, then the solid was calcinated in muffle furnace at 600 °C for 5 h.

2.4 Synthesis of NiO Powder

In first the NiO were synthesized by 0.005 molar Nickel nitrate ($Ni(NO_3)_2$) was dissolved in 100 ml of distilled water.

In separate beaker 2.50 g of citric acid ($C_6H_8O_7$) was taken and dissolved in 50 ml of water and stirred well. The Citric acid solution was added to the nickel nitrate dissolved solution by slowly. After homogenization of the solution, the pH range was reached upto 8 by aqueous NH_3 solution was added dropwise. Heated the solution slowly in 70 °C and evaporated. After the material was kept into an oven at 100 °C for dried the water. Then the gel was calcinated in muffle furnace at 500 °C for 5 h.

2.5 Preparation of $CuTiO_3$/ZnO Binary Composites

In the preparation of 2wt % $CuTiO_3$/ZnO binary composites, 0.02 g of $CuTiO_3$ was first dispersed in 40 ml of CH_3CH_2OH, 0.2750 g of oxalic acid was added to that suspension, and the mixture was stirred in a magnetic stirrer to form a homogeneous suspension. Further 0.98 g of ZnO was added, and the stirring was continued to overnight and then the suspension was dried and then annealed at 300 °C for 3 h in a muffle furnace. The same procedure used for synthesis of further heterojunction photocatalysts (4wt% $CuTiO_3$/ZnO, 6wt% $CuTiO_3$/ZnO, 8wt% $CuTiO_3$/ZnO, 10wt% $CuTiO_3$/ZnO and 8 wt % NiO/ZnO heterojunction semiconductor) and were labelled as CuZ4, CuZ6, CuZ8, CuZ10 and NZ 8 respectively.

2.6 Synthesis of NiO/$CuTiO_3$/ZnO Ternary Composites

The terrnary composites of NiO/$CuTiO_3$/ZnO photocatalysts are prepared as follows: prepared $CuTiO_3$/ZnO binary composite was weighed 0.98 g and it dispersed in 40 ml of ethanol and stirred in magnetic stirrer for 1 h. To the above solution 0.02 g of Nickel oxide powder was added and again stirred continuously up to twelve hours. Then the mixture was dried at 80 °C in the air, the ethanol was volatilized and volatilized powder annealed at 300 °C for 3 h in a muffle furnace. That obtained dark greenish powder is the ternary composites NiO/$CuTiO_3$/ZnO. Further, NiO/$CuTiO_3$/ZnO ternary composites are prepared with various weight ratio of NiO and $CuTiO_3$/ZnO, these ternary composites labeled as 1NCZ, 2NCZ, 3NCZ, 4NCZ and 5NCZ.

2.7 Photocatalytic Degradation of NiO/$CuTiO_3$/ZnO Ternary Composites

The photocatalytic experiments of on clear sky days during the period of October–December–2020. First, 50 ml of dye solution was diluted (concentration 50 mg l^{-1}) and added 2 to 3 drops of 1 mol HCL in a 250 ml beaker and added 50 mg of prepared photocatalyst. That dye solution was kept under direct sunlight with continuous aeration and the concentration of the dye remains was measured periodically by measuring its light absorbance at the visible λ_{max} by using Elico SL-171 Visible spectrophotometer. So as to keep away from the deviation in results because of fluctuation in the intensity of the sunshine, a set of experiments have been carried out at the same time. The photocatalytic active species, detected via using in the similar process in presence of scavengers.

2.8 Characterization of Photocatalyst

X-ray powder diffraction (XRD) patterns of the photocatalysts were recorded on a Philips X'pert-MPD diffractometer in the 2 h range 20°–80° using Cu Kα radiation. The data were collected with a step of 0.028 (2 h) at room temperature. The phase structure of the products was determined by comparing the experimental X-ray powder patterns to the standard compiled by the Joint Committee on Powder Diffraction and Standards (JCPDS). The crystalline sizes were calculated from the peak breadth via the Scherrer equation. The surface morphologies and particle size were observed by Scanning Electron Microscopy (JEOL.JSM-6360LV). The optical properties of the synthesized catalysts were measured by using UV–Vis DRS spectrophotometer (Shimadzu, UV-3600) with $BaSO_4$ as the background. The photoluminescence emission spectra of the samples were measured at room temperature via Perkin-Elmer LS 55 Luminescence spectrophotometer. Fourier transform infrared spectra of the samples were measured on an IR Prestige-21 spectrometer (Shimadzu). For this, the samples were formed into pellets with KBr.

3 Results and Discussion

3.1 Crystalline Property Analysis

The XRD patterns of the NCZ semiconductor heterojunction showed the presence of ZnO, $CuTiO_3$ and NiO with its hexagonal, monoclinic and cubic structures. The diffraction patterns of pure hexagonal wurtzite ZnO, monoclinic $CuTiO_3$ and cubic NiO exactly matches in the corresponding JCPDS card numbers are 36-145,73-6023 and 01-071-1179, respectively. From the peaks, diffraction peaks were not observed which indicates that there is no impurity in NCZ heterojunction, helps in the successful fabrication of the NCZ heterojunction (Fig. 1). This helps to confirms that the individual semiconductors do not react with each other [32]

The diffraction patterns of ternary NCZ heterojunction crystallanity might be decreased. The decreased crystalline phase of ZnO indicates NiO cover over the surface of $CuTiO_3$/ZnO binary heterojunctions.

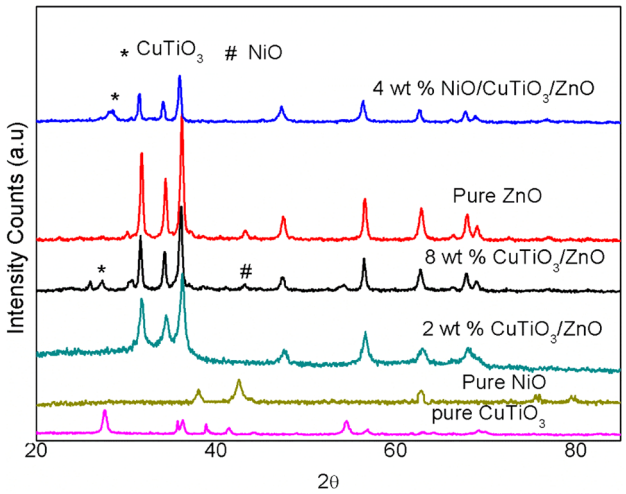

Fig. 1 XRD patters of Pure ZnO, $CuTiO_3$, NiO and 8 wt% $CuTiO_3$/ZnO, 4 wt% NiO/$CuTiO_3$/ZnO ternary composites

3.2 Formation and Morphology of ZnO Microstructure

Scanning electron microscopic analysis was used to study the morphology and size of the photocatalysts. The SEM of pure ZnO, 8 wt% $CuTiO_3$/ZnO, 3 wt% NiO/$CuTiO_3$/ZnO, 4 wt% NiO/$CuTiO_3$/ZnO and 5 wt% NiO/$CuTiO_3$/ZnO ternary composites are display in Fig. 2. The morphology of pure ZnO (Fig. 2a) reveals small particles with highly agglomerated in nature. While binary photocatalysts such as 8 wt% $CuTiO_3$/ZnO, Fig. 2b displays the "un desired morphology" due to the agglomerated surface, which reveal that the binary heterojunction arehjkj interconnected and large particle are formed between the adjacent particles, Fig. 2c show as after thermal treatment binary photocatalyst are loose and soft agglomerates owing to the granules-on-granules structure, which have a tendency to twist to minimize the surface energy. Figure 2d, show that NiO particles are physically anchored on to the $CuTiO_3$/ZnO surface and have formed a good crystalline ternary heterojunction structure, this type of morphology helps in photogenerated charge separation. Further increase the NiO content on $CuTiO_3$/ZnO surface (Fig. 2e) the particles get aggregate with irregular particle size. So that these type of surface morphology do not support better photocatalytic performance.

3.3 Optical Property

Figure 3 exhibits the photoresponse evolution of the ternary composites after inclusion of NiO on $CuTiO_3$/ZnO. The ternary composites slowly altered from white (pure ZnO) to dark grey (NiO/$CuTiO_3$/ZnO). This phenomenon indicates absorbance band shifted to visible light region. According to Kubelka–Munk function, the band-gap widths (Fig. 3c) of the samples were calculated to be 3.19, 3.01, 3.48, and 3.1 eV, 3.4 eV and 3.0 eV, 2.95 eV, 2.90 eV for ZnO, $CuTiO_3$, NiO and 8 wt% $CuTiO_3$/ZnO, 8 wt% NiO/ZnO and 3 wt% NiO/$CuTiO_3$/ZnO, 4 wt% NiO/$CuTiO_3$/ZnO and 5 wt% NiO/$CuTiO_3$/ZnO ternary heterojunctions. NiO and $CuTiO_3$ has reduced band-gap because of the lower incident energy caused by electrons, thereby reinforcing the visible light utilization efficiency.

3.4 Photoluminescence Study

In the Photoluminescence (PL) the recombination of photogenerated charge carriers emit the light. The photo-generated charge separation phenomenon of pure ZnO, 8 wt% $CuTiO_3$/ZnO, 8wt% NiO/ZnO binary composites and different weight ratio of ternary NiO/$CuTiO_3$/ZnO semiconductor heterojunction were examined by PL spectra, as shown in Fig. 4. In pure ZnO due to the oxygen vacancies in ZnO powder shows the highest photoluminescence intensity. The recombination of photogenerated electron and hole pairs can delayed due to photo generated electrons effectively trapped, while the PL intensity in ternary NiO/$CuTiO_3$/ZnO heterojunction is relatively low compared to pure ZnO powder.

The optical and electrical property of ZnO by synergistic effects of NiO and CuTiO3 reduces theband-gap width of ZnO and enhancing the visible light absorption and another one improving both UV and visiblelight responses.

3.5 Molecular Confirmation of Photocatalyst

Fourier transform infrared spectroscopy (FTIR) was used to identify the characteristic functional groups in the as-prepared microstructure composites. The samples are dried and mixed with KBr to form pellets, which were then analyzed by FTIR. The FTIR spectrum of ZnO, 8 wt% $CuTiO_3$/ZnO, and 5 wt% NiO/$CuTiO_3$/ZnO ternary composites is displayed in Fig. 3. The peaks around 400–700 cm^{-1} arise because of M–O and O–M–O vibrations [34]. In Fig. 5a indicates FTIR spectrum of ZnO powder. In this spectrum, a characteristic broad band obtained nearly 625 cm^{-1}, its specifically indicate Zn–O vibrations. The characteristic peaks near 621 and 670 cm^{-1} (Fig. 5b and c), can be attributed to the Cu–O and Ni–O–Zn or Cu–O–Zn stretching modes of vibrational frequencies of metals interlinked by common oxygen atoms. There is no C=O stretching band observed around ~ 1632 cm^{-1} in Fig. 5b and C, which means all oxalic acid were removed in the composite samples after calcinations process.

The FTIR spectrum of a photocatalysts shows broad absorption bands between 2800 and 4000 cm^{-1}, mainly ascribed to OH− vibration from the hydroxyl group, which is probably attributed to the adsorbed water on the surface of

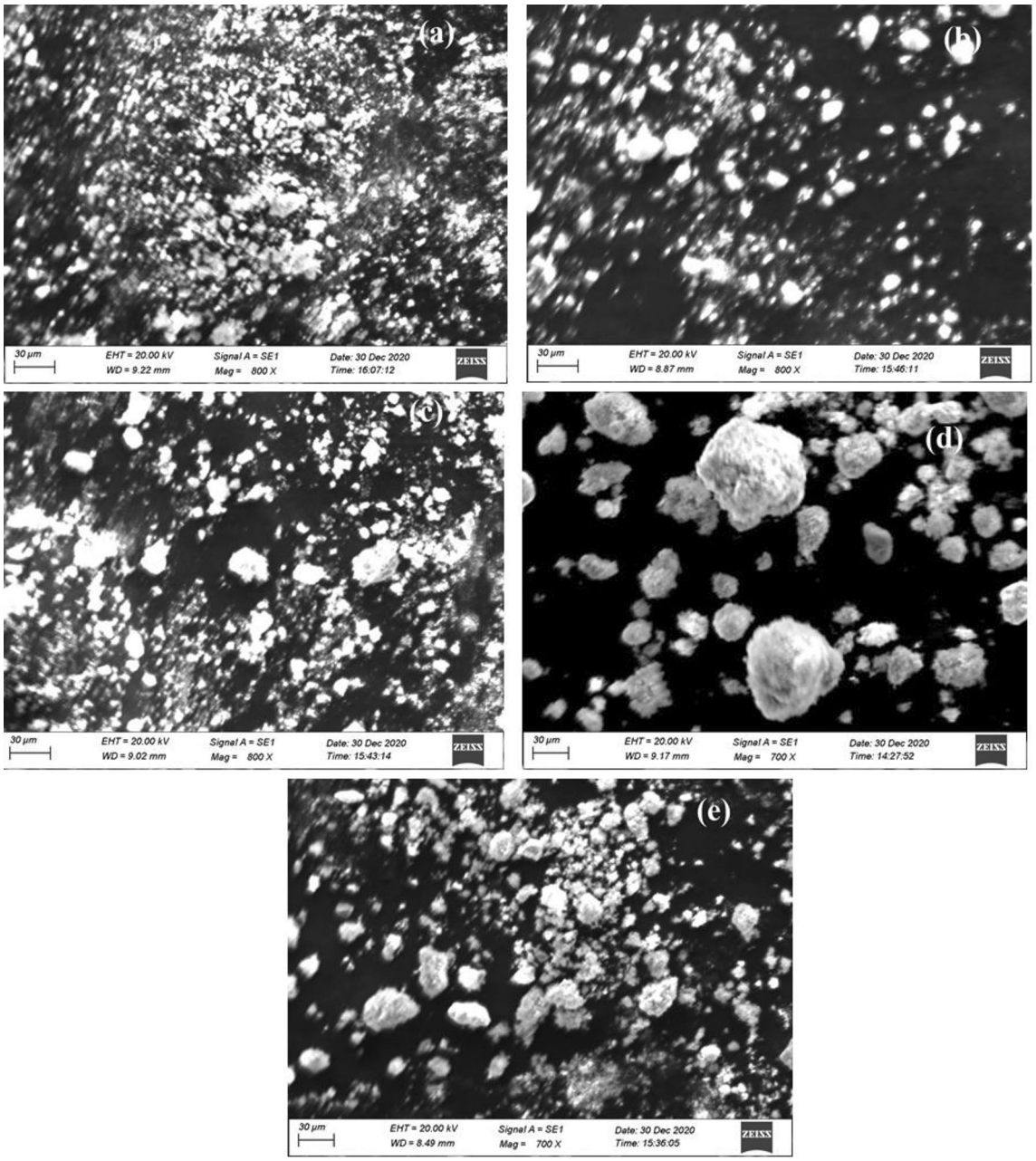

Fig. 2 SEM images of pure ZnO 8 wt% $CuTiO_3$/ZnO, 3 wt% NiO/$CuTiO_3$/ZnO, 4 wt% NiO/$CuTiO_3$/ZnO and 5 wt% NiO/$CuTiO_3$/ZnO ternary composites

the photocatalysts [33]. The hydroxyl groups helps in trapping the holes under sunlight irradiation to form hydroxyl radicals which helps to increase the photocatalytic effectiveness [33].

3.6 Effect of pH of the Dye Solution on 4NCZ

In Fig. 6, shows that the pH range 3–12 were used for photodegradation of RO 30 in the presence of 4NCZ (88% ZnO)0.50 mg/l concentration of dye and 0.5 mg/l of photocatalyst was used which shows that the pH range 3–7 has the positively charged 4NCZ heterojunction and the negatively charge RO 30 should readily attract each other, while they should repulse each other when pH is above 7 due to both are RB 30 and 4NCZ shows negative charge. The degradation rate of 4NCZ semiconductor photocatalysts was high at around pH 5. The ultimate reason is semiconductor photocatalysts are positively charged at pH bellow 7 and the RO 30 has been negatively charged species. At pH 7 they repulse each other and readily attract

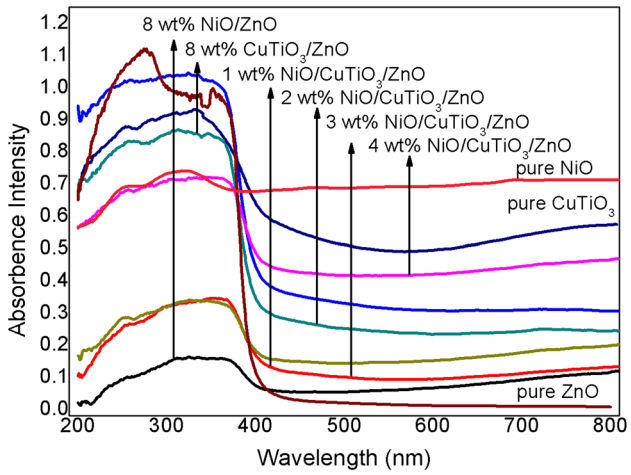

Fig. 3 UV–visible diffused reflectance spectra of pure ZnO, $CuTiO_3$, NiO 8 wt% $CuTiO_3$/ZnO, 3 wt% NiO/$CuTiO_3$/ZnO, 4 wt% NiO/$CuTiO_3$/ZnO and 5 wt% NiO/$CuTiO_3$/ZnO ternary composites

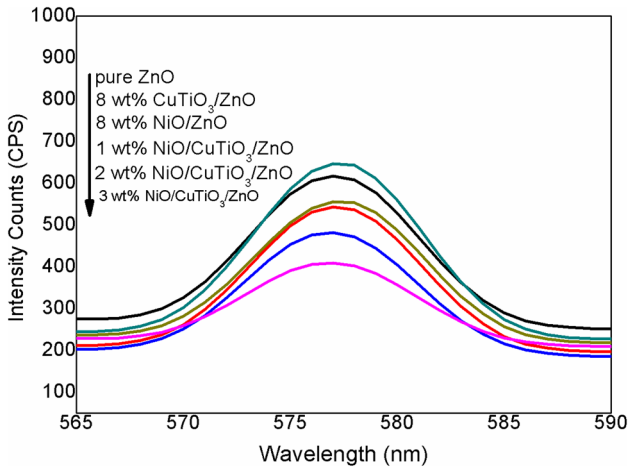

Fig. 4 Photoluminescence spectra of photocatalysts

each other due to both are RB 30 and 4NCZ shows negative charge.

The 4NCZ at extreme pH values, such as pH 3 and 12 gets readily dissolved. ZnO photocatalyst reveal a propensity to dissolve at acidic and basic environment,:

Therefore, the decreased photocatalytic activity at low and higher pH values can be attributed to the dissolution in strong acidic or alkaline environment.

3.7 Photocatalytic Performance of the Developed NiO/$CuTiO_3$/ZnO Semiconductor Heterojunction

3.7.1 Photocatalytic Activity

Photocatalysis is the process of conversion of solar energy to solve the environmental pollution. Solar energy is providing energy in nature which has 4% of solar radiation in the UV region and 46% in visible light, enhances the photocatalytic activity of the semiconductors. To study the photocatalytic degradation efficiency of the ternary NiO/$CuTiO_3$/ZnO heterojunction system, RO 30 solution as a model dye effluent under irradiation with solar lights are evaluated for the degradation. Dye molecules needs 20 min to reach an adsorption–desorption equilibrium. In this work, RO 30 a typical dye pollutant, with absorption at 430 nm, used for photocatalytic activity under solar light irradiation.

3.7.2 Effect of $CuTiO_3$ Coupling on ZnO Photocatalyst Powder

The apparent first order rate constants of the binary $CuTiO_3$/ZnO heterojunction with different weight contents of ZnO and $CuTiO_3$ under solar light irradiation was showed in Fig. 7. Figure 7a demonstrates that the degradation rates increased with the increasing $CuTiO_3$ adding from 2 to 10 in the weight ratio. $CuTiO_3$ coupling above 8 wt% decrease the degradation rate which results in the optimum photocatalytic activity for binary heterojunctions at a $CuTiO_3$: ZnO weight ratio of 0.8:0.92. The higher photocatalytic activity of $CuTiO_3$ coupling was due to the interfacial charge transfer and sustained charge carriers for long lifetime.

If there is high $CuTiO_3$contentsphotocatalytic activity would be decreased because lack of electron–hole charge separation and an increase in the (e^-–h^+) recombination rate [35, 36].

3.7.3 Effect of Ternary Heterojunctions Formation

The binary and ternary heterojunctions photocatalytic performance was shown in Fig. 8. The degradation of RO 30 under natural solar light irradiation was studied. The photocatalytic activity of pure photocatalysts such as NiO, $CuTiO_3$ and ZnO are compared with binary and ternary heterojunctions. Moreover, in Fig. 7b, the ternary NiO/$CuTiO_3$/ZnO heterojunction exhibited higher photomineralization capability than both the binary and unary photocatalysts. The ternary NiO/$CuTiO_3$/ZnO heterojunction degraded something like 100% of the RO 30dye solution at 110 min, while the binary $CuTiO_3$/ZnO heterojunctions degraded about at 150 min. The RO 30 degradation using ternary NiO/$CuTiO_3$/ZnO heterojunction was due to the continuation of heterojunctions between NiO, ZnO

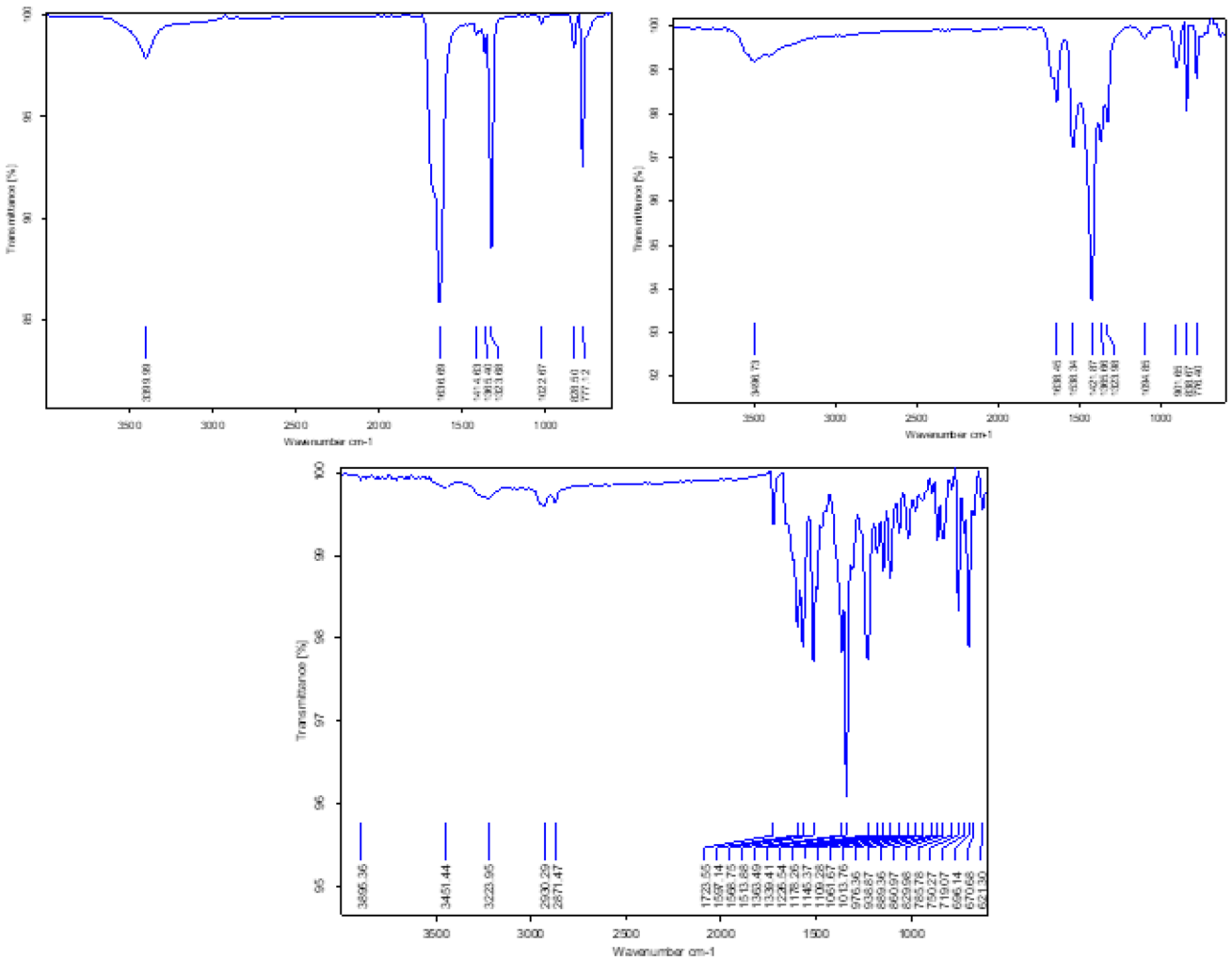

Fig. 5 FTIR spectra of ZnO, 8 wt% $CuTiO_3$/ZnO, and 5 wt% NiO/$CuTiO_3$/ZnO ternary composites

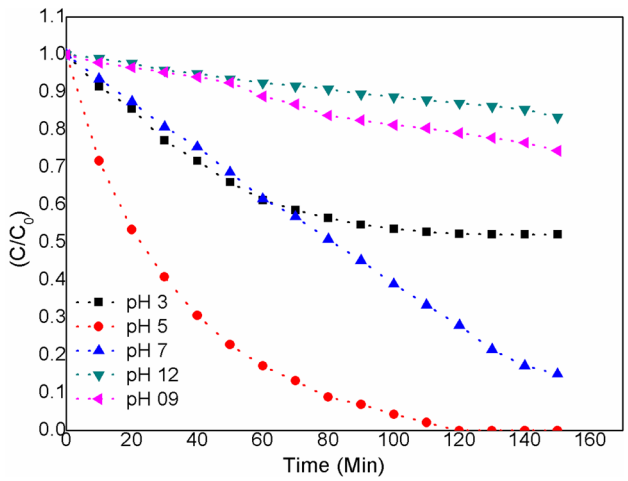

Fig. 6 Effect of pH of the dye solution on 4 wt% NiO/$CuTiO_3$/ZnO

and $CuTiO_3$, which prevent charge-carrier recombination than those in binary $CuTiO_3$/ZnO heterojunction. Due to this development larger surface area of the ternary NiO/$CuTiO_3$/ZnO heterojunction compared to those of the binary $CuTiO_3$/ZnO heterojunction, it exhibits the NiO has a smaller electron–hole diffusion length than the $CuTiO_3$/ZnO heterojunction systems and ZnO.

The degradation studies were analysed with the Langmuir–Hinshelwood kinetic model:

$$r_s = \frac{kKc}{1 + KC}$$

where r_S is the specific degradation reaction rate the dye (mgl^{-1} min^{-1}), C the concentration of the dye (mgl^{-1}), k the reaction rate constant (min^{-1}) and K is the dye adsorption constant. When the concentration (C) is small enough, the above equation can be simplified in an apparent first-order equation:

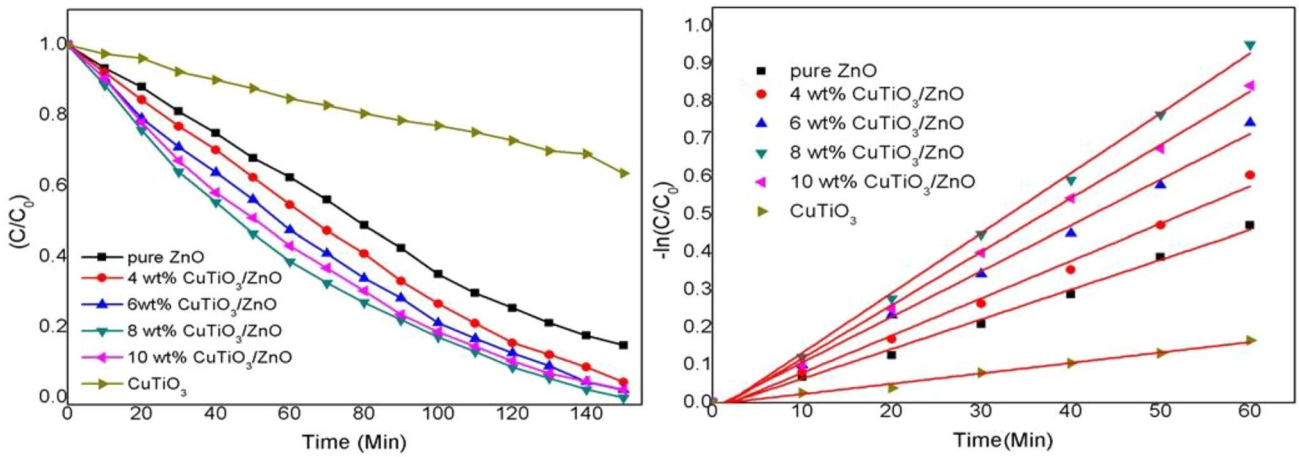

Fig. 7 **a**, **b** Kinetics of degradation of Reactive Orange 30 over ZnO, $CuTiO_3$ and binary $CuTiO_3$/ZnO heterojunction (initial concetration $C_0 = 50\ mgl^{-1}$)

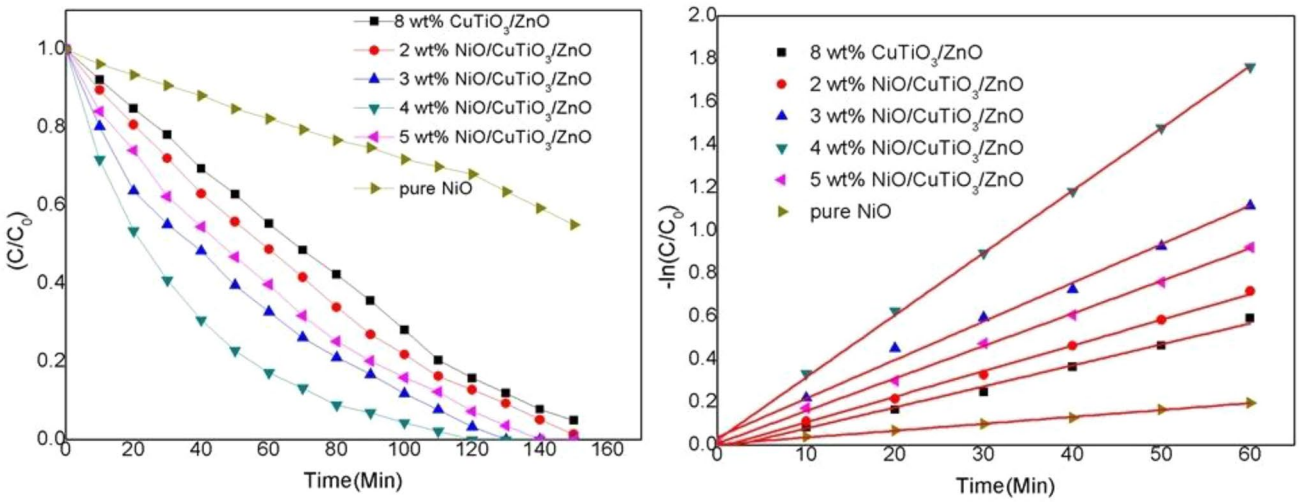

Fig. 8 **a**, **b** Kinetics of degradation of Reactive Orange 30 over NiO and ternary NiO/$CuTiO_3$/ZnO heterojunction (initial concetration $C_0 = 50\ mgl^{-1}$)

$$r_s = kKC = K_{app}C\left(= -\frac{dc}{dt}\right)$$

After integration, we will get

$$-\ln\left(\frac{C}{C_0}\right) = K_{app}t$$

where C_0 is the initial concentration (mg l^{-1}), C is the concentration of the dye after (t) minutes of illumination. The data obtained from the degradation of RO 30 fits well the apparent first order kinetics (Figs. 7b and 8b). The electrons transferred to surface adsorbed oxygen molecules and form superoxide anions, again transform to $OH^{\bullet}$ and degradation of RO 30 initiated.

3.7.4 Photocatalytic Mechanism

We proposed a mechanism for the degradation of reactive orange 30 onternary NiO/$CuTiO_3$/ZnO heterojunction under solar light irradiation as shown in Fig. 9. The electron injection from$CuTiO_3$to ZnO and hole were separation from ZnO to $CuTiO_3$semiconductor was studied. $CuTiO_3$ semiconductor can quickly excited electrons and transferred to a ZnO, conduction band of $CuTiO_3$has negative potential than ZnO. In our study $CuTiO_3$ coupled with ZnO system, has a important role in improving feeding of electron and extends ZnO by solar activity. The electrons are then scavenged by molecular oxygen O_2 to yield the

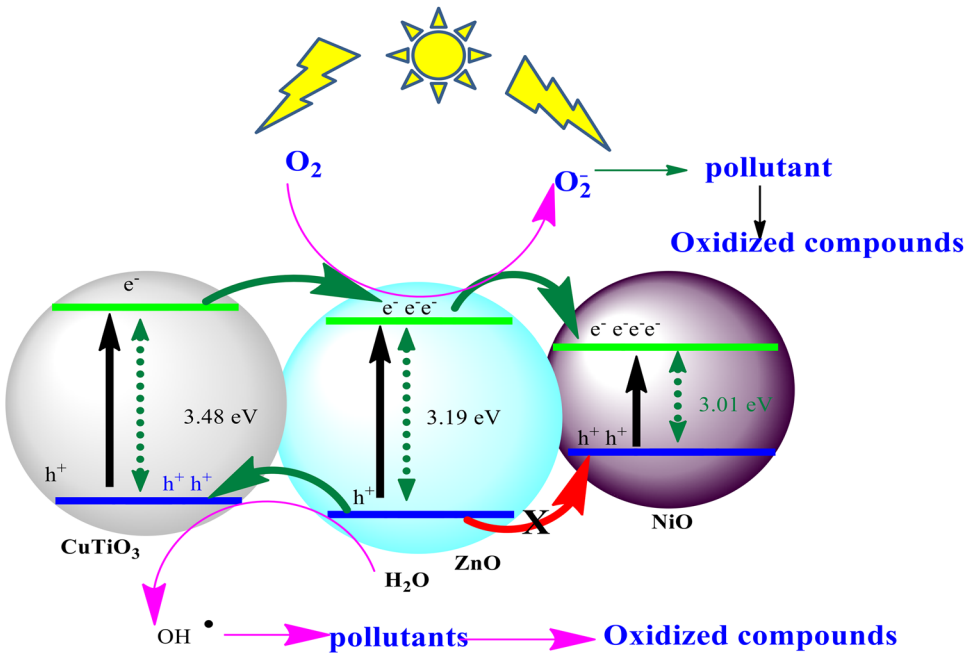

Fig. 9 Photoelectron injection mechanism proposed on ternary NiO/$CuTiO_3$/ZnO heterojunction

superoxide radical anion O^{2-}. It is might bea powerful reducing agent capable of degrading most pollutants.

However, the photo-generated electrons in ZnO cannot completely reduce O_2 to O^{2-} due to its band gap energy (3.19 eV). So that this imbalance activity will be managed by NiO Coupled with $CuTiO_3$/ZnO binary heterojunction..As shown in Scheme, the combination of NiO and $CuTiO_3$/ZnO binary heterojunction, photocurrent is formed by transfer of e^- from ZnO to theNiO when exposed to solar light. It prevents the e^- and h^+ from recombination. Finally important point out that the transfer of electron from $CuTiO_3$and ZnO is possible by photo-oxidizing power. Thus, the ternary NiO/$CuTiO_3$/ZnO heterojunction system is a promising method for the practicability of ternary NiO/$CuTiO_3$/ZnO heterojunction.

The valuable photocatalytic mechanism is depending on the configuration of active species. To analyze the degradation mechanism, radical trapping experiments were carried out to study the probable contribution from various active species towards the degradation of the RO 30. The radical scavenging experiments are shown in Fig. 10. In this technique, oxalic acid (OA), ascorbic acid (AA) and 2-propanol (2P) was introduced as hole, superoxide radical and hydroxyl radical scavenger, respectively. These three particular quenchers were selected based on the fact that for degrading organic pollutants, hole, superoxide, and hydroxyl radicals play a important role insolar light irradiation [37]. For comparison purpose, another experiment was performed with no scavenger (NS).

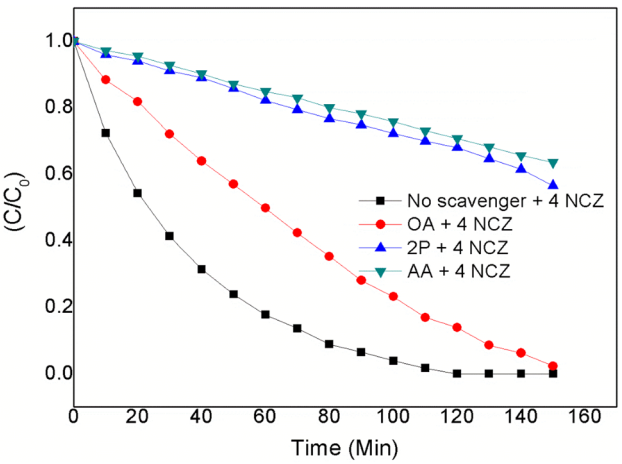

Fig. 10 Effect of scavengers on photocatalytic degradation using NiO/$CuTiO_3$/ZnO

As shown in the Fig. 10, in the absence of any scavenger ~ 98% degradation of RO 30 was achieved, while 36% degradation was found with ascorbic acid and 44% with 2-propanol respectively.

This results indicates that both superoxide and hydroxyl radicals plays an important role in the degradation process. Quenching effect was observed in the presence of Oxalic acid, introduction of oxalic acid degradation of RO 30 was potentially reduced to 96%. It was concluded that be hole was minorly responsible for the photocatalytic degradation of RO 30.

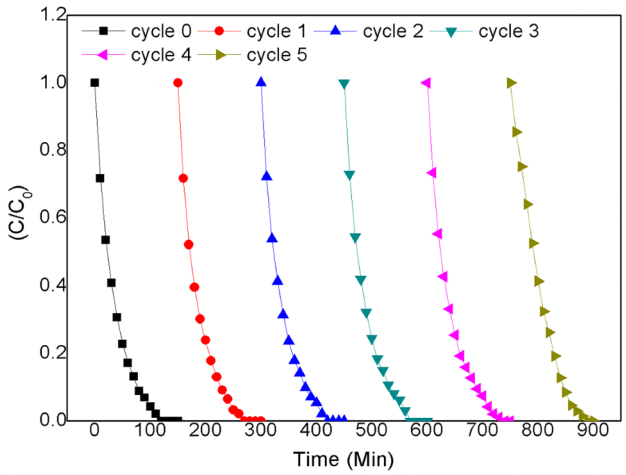

Fig. 11 Photocatalytic stability of 4NCZ ternary heterojunction

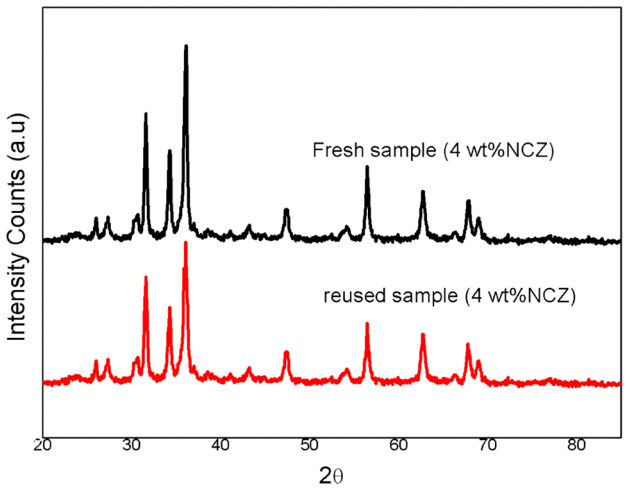

Fig. 12 XRD pattern of pure 4 wt% NCZ and reused 4 wt% NCZ composite

3.8 Stability and Reusability

To confirm the stability of ternary NiO/$CuTiO_3$/ZnO heterojunction during photocatalytic reaction, under solar light radiation repeated degradation of RO 30 for five times by cycling test was carried out. In Fig. 11, the photocatalytic activity of ternary NiO/$CuTiO_3$/ZnO semiconductor heterojunction is high even with third cycles. Further, the degradation rate was slightly decreased, due to the loss and catalytic poisoning of the photocatalyst during the recycling experiments.

Figure 12 shows the XRD patterns of the ternary NiO/$CuTiO_3$/ZnO heterojunction before and after photocatalytic reaction, and there is no observable structural difference in the samples before and after the reaction, indicating that the phase and structure of ternary NiO/$CuTiO_3$/ZnO heterojunction are stable during the photocatalytic reactions. But the intensity of main diffraction pattern decreased due to accumulation of degraded intermediates [38]. From the results it indicates that prepared heterojunction catalysts are stable and reusable for photocatalytic reactions.

4 Conclusions

Ternary NiO/$CuTiO_3$/ZnO semiconductor heterojunction were prepared with different weight ratios of NiO and $CuTiO_3$ for the degradation of RO 30. The XRD results proved good agreement with coupling of NiO, $CuTiO_3$ and ZnO composites. The absorption boundary of the NiO/$CuTiO_3$/ZnO semiconductor heterojunction shifted a lot to longer wavelengths compared to binary and pure ZnO. The recombination of photogenerated electron–hole pairs has been diminished in the modification ZnO by formation ternary structure; it is confirmed by PL spectra. All the NiO/$CuTiO_3$/ZnO ternary heterojunction showed excellent photocatalytic behavior than that of binary heterojunction and degradation of RO 30 under solar light irradiation. These results point out that the formation of heterojunction with close contacts between NiO and $CuTiO_3$/ZnO results in the easier charge transfer and more efficient separation of hole. Recyclic experiments specify the reusability and stability of NiO/$CuTiO_3$/ZnO semiconductor heterojunction. The study on the photocatalytic degradation pathway of the NiO/$CuTiO_3$/ZnO semiconductor heterojunction implies that O_2^{2-} and·OH radicals to be the main active species involved in the degradation process. Based on the band potential structure, a possible photocatalytic mechanism of NiO/$CuTiO_3$/ZnO semiconductor heterojunction under solar light irradiation was proposed.

References

1. A.B. Albadarin, M.N. Collins, M. Naushad et al., Activated lignin-chitosan extruded blends for efficient adsorption of methylene blue. Chem. Eng. J. **307**, 264–272 (2017)
2. S.M. Alshehri, M. Naushad, T. Ahamad et al., Synthesis, characterization of curcumin based ecofriendly antimicrobial bio-adsorbent for the removal of phenol from aqueous medium. Chem. Eng. J. **254**, 181–189 (2014)
3. M. Naushad, T. Ahamad, B. Al-Maswari et al., Nickel ferrite bearing nitrogen-doped mesoporous carbon as efcient adsorbent for the removal of highly toxic metal ion from aqueous medium. Chem. Eng. J. **330**, 1351–1360 (2017)
4. G. Piotrowska, B. Pierozynski, Electrodegradation of phenol through continuous electrolysis of synthetic wastewater on platinized titanium and stainless steel anodes. Int. J. Electrochem. Sci. **12**, 4444–4455 (2017)
5. A. Bódalo, E. Gómez, A.M. Hidalgo et al., Nanofltration membranes to reduce phenol concentration in wastewater. Desalination **245**, 680–686 (2009)

6. A. Kumar, F.J. Stadler, G. Sharma et al., Wide spectral degradation of Norfloxacin by Ag@$BiPO_4$/BiOBr/$BiFeO_3$ nano-assembly: Elucidating the photocatalytic mechanism under diferent light sources. J. Hazard. Mater. **364**, 429–440 (2019)
7. D. Zhao, J. Zhou, N. Liu, Characterization of the structure and catalytic activity of copper modifed palygorskite/TiO_2 (Cu2+-PG/TiO2) catalysts. Mater. Sci. Eng. A **431**, 256–262 (2006)
8. X. Zeng, Z. Wanga, W. Gen et al., Highly dispersed TiO2 nanocrystals and WO3 nanorods on reduced graphene oxide: Z-scheme photocatalysis system for accelerated photocatalytic water disinfection. Appl. Catal. B Environ. **218**, 163–173 (2017)
9. Y. Xu, Simple synthesis of ZnO nanofowers and its photocatalytic performances toward the photodegradation of metamitron. Mater. Res. Bull. **76**, 235–239 (2016)
10. S. Nagamine, K. Inohara, Photocatalytic microreactor using anodized TiO_2 nanotube array. Adv. Powd. Tech. **29**(12), 3100–3106 (2018)
11. A. Pruna, Z. Wu, J.A. Zapien et al., Enhanced photocatalytic performance of ZnO nanostructures by electrochemical hybridization with graphene oxide. Appl. Surf. Sci. **441**, 936–944 (2018)
12. H. Wang, S. Baek, J. Lee et al., High photocatalytic activity of silver-loaded ZnO-SnO2 coupled catalysts. Chem. Eng. J. **146**(3), 355–361 (2009)
13. S. Yan, Z. Liu, X. Wei et al., Preparation and photoelectrochemical properties of CdS nanoparticles using supercritical carbon dioxide. J. Nanosci. Nanotech. **16**(7), 7203–7209 (2016)
14. E. Soignard, D. Machon, P.F. McMillan et al., Spinel-structured gallium oxynitride (Ga3O3N) synthesis and characterization: an experimental and theoretical study. Chem. Mater. **17**(22), 5465–5472 (2005)
15. J.H. Li, R.Y. Hong, M.Y. Li et al., Effects of ZnO nanoparticles on the mechanical and antibacterial properties of polyurethane coatings. Prog. Org. Coat. **64**(4), 504–509 (2009)
16. R.Y. Hong, H. Li, L.L. Chen et al., Synthesis, surface modification and photocatalytic property of ZnO nanoparticles. Powd. Tech. **189**(3), 426–432 (2009)
17. P. Zhang, R.Y. Hong, Q. Chen et al., On the electrical conductivity and photocatalytic activity of aluminumdoped zinc oxide. Powd. Tech. **253**(2), 360–367 (2014)
18. S. Singhal, S. Dixit, A.K. Shukla, Self-assembly of the Ag deposited ZnO/carbon nanospheres: a resourceful photocatalyst for efficient photocatalytic degradation of methylene blue dye in water. Adv. Powd. Tech. **29**(12), 3483–3492 (2018)
19. W. Han, L. Ren, X. Qi et al., Synthesis of CdS/ZnO/graphene composite with high-efficiency photoelectrochemical activities under solar radiation. Appl. Surf. Sci. **99**, 12–18 (2014)
20. Z. Peng, Z. Jinteng, J. Jingjing, W. Hongtao, X. Tengfeng, L. Yanhong, Synthesis and study on Photogenerated charge behavior of novel Pt/CeO_2/ZnO ternary composites with enhanced photocatalytic degradation activity. J. Inorg. Organomet. Polym. Mater. **30**, 1589–1599 (2020)
21. A.I. Vaizoğullar, Ternary CdS/MoS_2/ZnO photocatalyst: synthesis, characterization and degradation of Of oxacin under visible light irradiation. J. Inorg. Organomet. Polym Mater. (2020). https://doi.org/10.1007/s10904-020-01563-0
22. T.B. Avis, S. Meera, O. Manaf, R. Antony, Heterostructured nanocomposites of Ag doped Fe_3O_4 embedded in ZnO for antibacterial applications and catalytic conversion of hazardous wastes. J. Inorgan. Organomet. Polym. Mater. **30**, 1944–1955 (2020)
23. S. Senobari, A. Nezamzadeh-Ejhieh, A comprehensive study on the enhanced photocatalytic activity of CuO-NiO nanoparticles: designing the experiments. J. Mol. Liq. **261**, 208–217 (2018)
24. C.J. Chen, C.H. Liao, K.C. Hsu et al., P-N junction mechanism on improved NiO/TiO_2 photocatalyst. Catal. Commun. **12**, 1307–1310 (2011)
25. M.A. Kanjwal, I.S. Chronakis, N.A.M. Barakat, Electrospun NiO, ZnO and composite NiO–ZnO nanofibers/photocatalytic degradation of dairy effluent. Ceram. Int. **41**, 12229–12236 (2015)
26. C. Li, C. Feng, F. Qu et al., Electrospun nanofibers of p-type NiO/n-type ZnO heterojunction with different NiO content and its influence on trimethylamine sensing properties. Sensor. Actuator. B Chem. **207**, 90–96 (2015)
27. M. Pirmoradi, S. Hashemian, M.R. Shayesteh, Kinetics and thermodynamics of cyanide removal by ZnO@NiO nanocrystals. Trans. Nonferrous Metals Soc. China. **27**, 1394–1403 (2017)
28. S. Mridha, D. Basak, Investigation of a P-CuO/N-ZnO Thin Film heterojunction for H_2 gas-sensor applications. Semicond. Sci. Tech. **21**, 928–932 (2006)
29. M. Mansournia, L. Ghaderi, CuO@ZnO Core-Shell nanocomposites: novel hydrothermal synthesis and enhancement in photocatalytic property. J. Alloy. Compd. **691**, 171–177 (2017)
30. Z. Jiang, D. Liu, D. Jiang et al., Heterojunction engineering of graphitic carbon nitride (g-C3N4) via Pt loading with improved daylight-induced photocatalytic reduction of carbon dioxide to methane. Dalton Trans. **43**, 13792–13802 (2014)
31. A. Anson-Casaos, I. Tacchini, A. Unzue et al., Combined modification of a TiO_2 photocatalyst with two different carbon forms. Appl Surf. Sci. **270**, 675–684 (2013)
32. S. Palla, Rav Gi, R. Velchuri et al., Photocatalytic degradation of organic dyes with Sn2+- and Ag+-substituted K3Nb3WO9(PO4)2 under visible light irradiation. Sci. Technol. **75**, 224 (2015)
33. A. Habibi-Yangjeh, M. Shekofteh-Gohari, Fe_3O=/ZnO/Ag_3VO_4/AgI nanocomposites: quaternary magnetic photocatalysts with excellent activity in degradation of water pollutants under visible light. Sep. Purif. Technol. **166**, 63–72 (2016)
34. C. Chen, Q.W. Liu, S. Gao et al., Fabrication of Ti^{3+} self-doped TiO_2(A) nanoparticle/TiO_2(R) nanorod heterojunctions with enhanced visible-light-driven photocatalytic properties. RSC Adv. **4**, 12098 (2014)
35. X. Tang, K.A. Hu, The formation of ilmenite $FeTiO_3$ powders by a novel liquid mix and H_2/H_2O reduction process. Mater J. Sci. **41**, 8025 (2006)
36. Y. Shavisi, S. Sharifnia, Z. Mohamadi, Solar-light-harvesting degradation of aqueous ammonia by CuO/ZnO immobilized on pottery plate: linear kinetic modeling for adsorption and photocatalysis process. J. of Env. Chem. Eng. **4**, 2736–2744 (2016)
37. R. Saravanan, S. Karthikeyan, V.K. Gupta, Enhanced photocatalytic activity of ZnO/CuO nanocomposite for the degradation of textile dye on visible light illumination. Mater. Sci. Eng. **33**, 91–98 (2013)
38. Y. Shi, D. Yang, Y. Li et al., Fabrication of PAN@ TiO_2/Ag nanofibrous membrane with high visible light response and satisfactory recyclability for dye photocatalytic degradation. Appl. Surf. Sci. **426**, 622 (2017)